Green Biosynthesis of CdS Nanoparticles Using Yeast Cells for Fluorescence Detection of Nucleic Acids and Electrochemical Detection of Hydrogen Peroxide

Huan Feng[1], Shi-yong Liu[2], Xiao-bing Huang[3], Ran Ren[4], Yan Zhou[3], Cai-ping Song[1*] and De-hui Qian[5*]

[1] Division of Nursing, Second Hospital Affiliated to Third Military Medical University. XinQiao Hospital, ChongQing 400037, China
[2] Department of Neurosurgery, Second Hospital Affiliated to Third Military Medical University. XinQiao Hospital, ChongQing 400037, China
[3] Department of Hepatobiliary Surgery, Second Hospital Affiliated to Third Military Medical University. XinQiao Hospital, ChongQing 400037, China
[4] Departement of Scientific Research, Second Hospital Affiliated to Third Military Medical University. XinQiao Hospital, ChongQing 400037, China
[5] Departement of Cardiology, Second Hospital Affiliated to Third Military Medical University. XinQiao Hospital, ChongQing 400037, China
[*]E-mail: qiandehui@163.com

In this work, a green method was reported to biosynthesize the CdS nanoparticles, where the yeast Saccharomyces cerevisiae was used as the nitrogen source. To characterize the as-prepared CdS NPs, UV-Vis spectroscopy, XRD and SEM were employed. The results indicated that the as-synthesized CdS NPs from Saccharomyces cerevisiae exhibited a mean size of 4.7 nm with high purity. The electrochemically detection of hydrogen peroxide and fluorescence-enhanced detection can be achieved by the application of biosynthesis CdS nanoparticles.

1. INTRODUCTION

As we know, science and technology of nanomaterials have attracted increasing attention in last two decades [1]. Producing the desired nanostructures is the foundation of nanotechnology. The

term nanomaterials refers to materials that have at least one dimension in the size ranging from 1 to 100 nm [2]. Different kinds of materials have been fabricated, which demonstrated different morphologies. Nanomaterials with different size, distribution and surface area demonstrate totally different physical, chemical and mechanical properties. Recently, the main ways of nanoparticle preparation are physical and chemical methods. However, physical and chemical methods are too limited due to the requirement of sophisticated instruments and toxic reagents. It is urgent to find an environmentally benign and cost-effective method to fabricate nanomaterials, which is helpful for their application.

Recently, biosynthesis of nanoparticles, which is simple, economical and nontoxic, has attracted much attention [3-7]. Furthermore, nanometer-sized semiconductor with unique properties, which is composed of binary chalcogenides belonged to groups II-VI, such as CdS, PbS and ZnS, has been considerably explored [8-10]. Meanwhile, owing to its wide application in field effect transistors, photovoltaics, photocatalysis, photoluminescence, infrared photodetectors, solar cells and lighting emitting diodes, extensive investigation about CdS, which is one of them, has been performed [11-15]. Utmost importance of life science is to quantitatively determine the micro amounts of nucleic acids [16, 17]. The fluorescence is frequently applied to direct in-situ assays due to its extremely sensitive and adaptable form. The fluorescent reporters about inorganic nanostructures such as gold nanoparticles are dominated in current research [18]. The well-defined CdS nanoparticles have developed as promising candidates as fluorescent probes, which demonstrate wide application in biological and medical issue such as bioassays, cell imaging and clinical diagnostics.. For instance, surface modified CdS nanoparticles as fluorescent probe for the selective detection of cysteine was reported by the Negi's group [19]. Meanwhile, a fluorescence probe for the ultrasensitive detection of DNA was observed in Wang's group [20].

Chemical method with the use of toxic reagent is widely to synthesize the CdS [21, 22]. It is essential to develop an economical and benign approach with absence of toxic chemicals in the synthesis protocol, which is to meet the requirement and exponentially increasing technological demand [23]. It is deep-rooted that Inorganic materials can be produced by many organisms both at the extra- and intracellular level [24, 25]. Herein, a biosynthesis method nanoparticles was reported to fabricate the CdS nanoparticles, where the yeast Saccharomyces cerevisiae was used. The as-prepared CdS nanoparticles can be characterized by some measurements, such as UV-vis spectroscopy, XRD and SEM. As an effective sensing platform, the biosynthesized CdS nanoparticles can be applied to fluorescence-enhanced nucleic acid detection. What's more, the hydrogen peroxide was electrochemically determined by using the biosynthesized CdS. nanoparticles.

2. EXPERIMENTS

2.1. Biosynthesis of CdS nanoparticles

Based on the method by Prasad et al [26], the biosynthesis of CdS was conducted with some modifications. Typically, 25% ethanol with nutrients was added to make the sample diluted four times

after 25 ml of yeast suspension filtered. The culture would attain a light straw color after grown for another 24 hours. Meanwhile, freshly as-prepared hydrogen sulfide with deionized water (30 ml) was sparged in the Kipp's apparatus for 5 minutes. Then, aqueous H_2S (5 ml) and 0.25M $CdCl_2$ (20 ml) solution were put into the solution until the color changed to deep orange yellow, which meant that the CdS was formed. For initiating the transformation, culture solution combined with CdS solution was heated to 60 ^oC in a steam bath for 30 minutes. Then, the solution of culture was cooled down and incubated overnight. The CdS nanoparticles were filtered before rinsed with water and ethanol.

2.2. Characterization

The XRD with Cu Kα radiation (D8-Advanced, Bruker, Germany) was employed to characterize the crystal phase information of the sample from 5 to 80 in 2θ. UV-vis spectrophotometer (HALO RB-10, Dynamica) was used for optical analysis. Transmission electron microscope (TEM, Hitachi H-7500, Japan) was taken to detect the morphology of CdS nanoparticles.

2.3. DNA detection

The following description is the procedure for detecting the DNA: Based on the changes of the fluorescence intensity in the whole system, the DNA can be detected by using CdS nanoparticles while added to CdS solution. Double-stranded DNA detaching from the CdS nanoparticles, which led to recover the fluorescence, was produced by the hybridization of the probe with its target. The following is the oligonucleotide sequences.

ECM dye-labeled single-stranded DNA (P_{HIV}): 5'-ECM-AGT CAG TGT GGA AAA TCT CTA GC-3'

Complementary target to P_{HIV} (T): 5'-GCT AGA GAT TTT CCA CAC TGA CT-3'

In a classic detection procedure, sample solution with different amounts of P_{HIV} and 20 ul of 0.2 mM CdS nanoparticles were added together into acetate buffer solution (3.0 ml, pH=0.91). Fluorescence at λ = 530 nm is measured for maximal synchronous intensity of the system. A specific amount of P_{HIV} (T) was put in the above mixture. After that, the intensity of recovery fluorescence at the same wavelength number was recorded.

2.4. Electrochemical determination of hydrogen peroxide

Electrochemical determination is performed with a three electrode system. Glassy carbon electrode modified by CdS nanoparticles was employed as working electrode, reference electrode was saturated Ag/AgCl electrode and Pt electrode is taken as counter electrode. GCE surface modification was performed as following description: before dried at room temperature, 0.5mg/ml of CdS nanoparticles solution (5 ul) was added dropwise on the GCE surface. The electrochemical impedance spectroscopy (EIS) is used to assess the electron transfer performance on the original and modified GCE electrodes. The experimental settings are specified as follows: The 10^1-10^5 Hz, 5 mV, 5 mM [Fe

$(CN)_6]^{3-/4-}$ and 0.1 M KCl represented frequency range, amplitude, probe and supporting electrolyte respectively. In order to determine the hydrogen peroxide by using CV method, san rates 50 mV/s ranging from 0 to 1.0 V and 0.1 M PBS (pH=7) were used.

3. RESULTS AND DISCUSSION

The UV-vis spectrum was taken to confirm the formation of CdS nanoparticle. Corresponding to energy gaps of 2.70 eV, a clear absorption edge was exhibited in this dispersion as shown in the Figure 1A, which demonstrated a considerable blueshift compared to the absorption band edge of bulk CdS. [26]. It is obvious that bulk materials have a narrower band gap than CdS nanoparticles due to the quantum confinement of electron-pair when absorbing a sufficiently energetic photo.
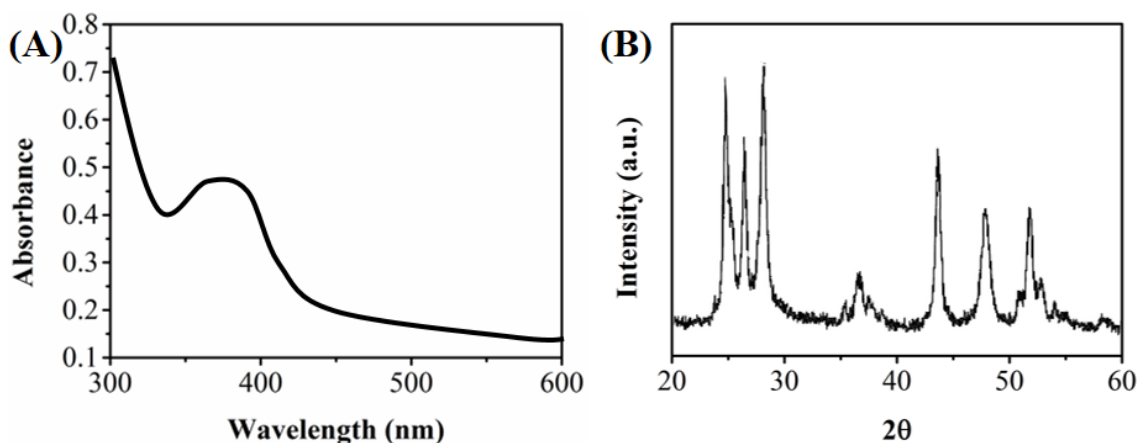

Figure 1. (A) UV-vis spectrum and (B) XRD pattern of biosynthesized CdS NPs.

The oxido-reductases and quinones in the membrane and cytosol of yeast were the keys to the formation of CdS nanoparticles. Depending on the pH condition, two different ways can be achieved when the oxido-reductases is available. At a high pH, the reductases can be activated while the activation of oxidases can be achieved at a low pH [27, 28]. Through the process of tautomerization, redox reaction can be facilitated by yeast. After H_2S reacted with the $CdCl_2$, the transformation of CdS nanoparticles happened suddenly, where the molecular oxygen for transformation, triggering low pH-sensitive oxidases and tautomerization of quinones were achieved. *Candida glabrata* cells was employed to observe the similar process [29]. Oxygenases can be harbored in the endoplasmic reticulum by the CdS nanoparticles after CdS entered into the cytosol, where the cellular level detoxification through the process of oxidation was the main target [30].

As shown in Figure 1B, it indicates the XRD pattern of as-biosynthesized CdS nanoparticles. the (100), (002), (101), (102), (110), (103), (200), (112), (201) and (004) phases of standard pattern of Hawleyite CdS (JCPDS 10-0454) represented the reflection peaks of the biosynthesized CdS NPs at 24.8^o, 26.7^o, 28.2^o, 36.8^o, 43.7^o, 47.6^o, 50.8^o, 51.6^o, 52.7^o respectively, the point that pure phase Hawleyite CdS was obtained was confirmed. It is worth to note that high purity CdS nanoparticles can

be produced by the proposed synthesis method, because there were no any impurities to be observed reflected by diffraction peaks.

TEM image of as-biosynthesized CdS nanoparticles is shown in the Figure 2A. Isolated nanoparticles with sphere morphology are illustrated by the micrographs. Meanwhile, morphology characterization also proved the excellent dispersion. The size distribution of the as-biosynthesized CdS nanoparticles is in the Figure 2B, where the average particle size is 2.76 nm with the distribution ranging from 0.5 to 4.5 nm.

The application of biosynthesized CdS NPs was studied by fluorescent detection of DNA. An oligonucleotide sequence associated with human immunodeficiency virus (HIV) labeled at the 5' end with the dye ECM was chosen as a model.
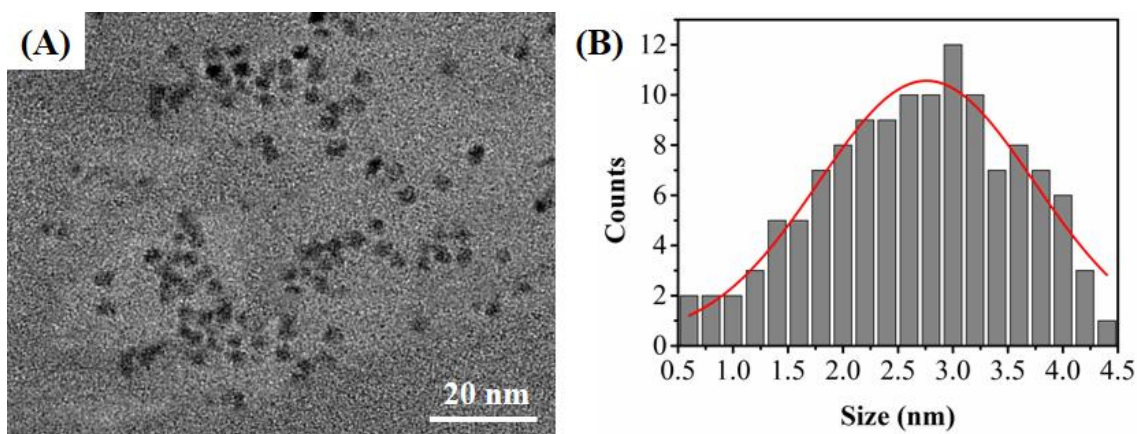

Figure 2. (A) TEM image and (B) size distribution of biosynthesized CdS NPs.
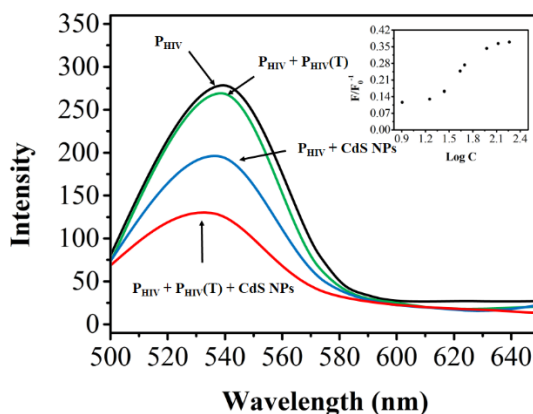

Figure 3. Fluorescence emission spectra of P_{HIV} (100 nM) with absence and presence of CdS NPs and $P_{HIV}(T)$. Inset: fluorescence intensity ratio of P_{HIV}-CdS NPs against logarithm of the concentration of $P_{HIV}(T)$. Excitation wavelength was at 470 nm, and the emission was monitored at 540 nm.

As shown in Figure 3, a strong fluorescence emission spectrum was recorded for the P_{HIV} (100 nM) due to the presence of the fluorescein-based dye. After addition of the CdS NPs, more than 40% of the fluorescence was quenched, suggesting the P_{HIV} was quenched effectively by adsorbed onto the

CdS NPs. On the other hand, the addition of complementary sequence P_{HIV} (T) (500 nM) showed little effect on the fluorescence of the P_{HIV}. In contrast, the addition of the P_{HIV} (T) into P_{HIV} with CdS NPs resulted in more than 70% fluorescence recovery. Because the CdS NPs exhibit no fluorescence emission at the recorded wavelength range, the measurement of the CdS-involved sample can be fully attributed to the concentration change of the target molecules. The inset in Figure 3A shows the relationship between the fluorescence intensity changes (F/F_0^{-1}) of P_{HIV}–CdS NP complexes and P_{HIV} (T) concentration, where F_0 and F represent the ECM fluorescence peak intensity in the absence and the presence of P_{HIV}(T), respectively. Based on a series of experiments, we found that the CdS NPs can effectively detect P_{HIV}(T) in the concentration range of 1 to 500 nM, suggesting that the CdS NPs are a suitable candidate for use as fluorescence probe. These promising results can be ascribed to the following reasons. The CdS NPs have a negative surface charge (measured as -10.2 mV), which promotes a stronger coordination interaction with the nitrogen atoms of P_{HIV} [31]. On the other hand, the CdS NPs do not interact with hybridized P_{HIV}(T) due to the absence of unpaired DNA bases. The detection of the P_{HIV}(T) was then divided into two steps. First, the dye labelled P_{HIV} was adsorbed onto the CdS NPs. Then, the addition of P_{HIV}(T) resulted in hybridization of the P_{HIV} and P_{HIV}(T), which disturbed the interaction between the P_{HIV} and the CdS NPs and led to the recovery of the fluorescence emission. The fluorescence intensity recovery percentage can be then used for calculated for estimating P_{HIV}(T) concentration.

The amount of CdS NPs used for DNA detection was optimized in this study. Figure 4 shows the fluorescence intensity recovery profiles using 0, 10, 20, 30 and 40 μL CdS NP dispersions (0.2 mM). As shown in the figure, the quenching efficiency showed a significant increase when the amount of CdS NPs was increased due to the strong absorption of the CdS NPs. However, the recovery was decreased when a large amount of CdS NPs was used. This is likely due to the adsorption of P_{HIV} on excessive numbers of CdS NPs, which could compete with the hybridization of P_{HIV} with P_{HIV}(T), resulting in an unfavorable recovery efficiency. Based on the experimental study, 20 μL of CdS NPs was used for DNA detection.
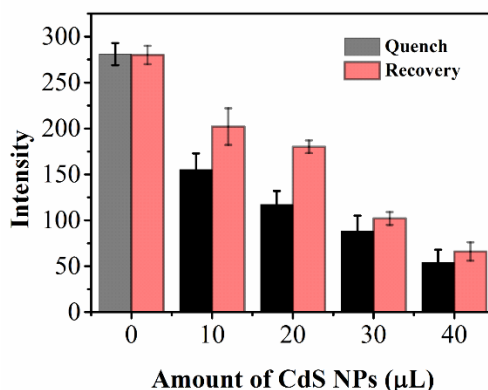

Figure 4. Fluorescence intensity histograms of P_{HIV}-CdS NPs and P_{HIV} + CdS NPs + P_{HIV}(T) with the using of 0, 10, 20, 30 and 40 μL CdS NPs.

To investigate the improvement of biosynthesized CdS NPs, cyclic voltammograms (CVs) for 1 mM H_2O_2 oxidation were obtained on CdS NPs/GCE, and the results were compared with that obtained on bare GCE and commercial CdS NPs/GCE (C-Cd/GCE). As can be seen from the curve obtained on bare GCE (Fig. 5A), no obvious oxidation peak was observed. In contrast, owing to the catalytic activity of CdS NPs, a well-defined oxidation peak was observed on C-Cd/GCE with the anodic peak potential at 0.86 V. As to the H_2O_2 oxidation on CdS NPs/GCE, an outstanding eletctrocatalytic performance was presented. An oxidation peak at 0.62 V was clearly observed in the process of 1 mM H_2O_2 oxidation on CdS NPs/GCE, as compared to the smooth CV curve of the CdS NPs/GCE in PBS. When CdS NPs/GCE was applied to the H_2O_2 oxidation, the current response was enhanced and the over-potential was lowered, demonstrating the excellent electrocatalytic property of biosynthesized CdS NPs that probably resulted from high specific surface area.
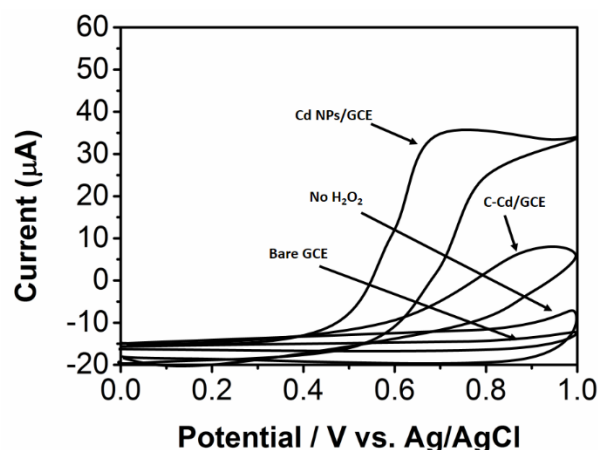

Figure 5. (A) CVs of Bare GCE, CdS NPs/GCE and C-Cd/GCE towards 1 mM H_2O_2 in 0.1 M PBS (pH 7.5).
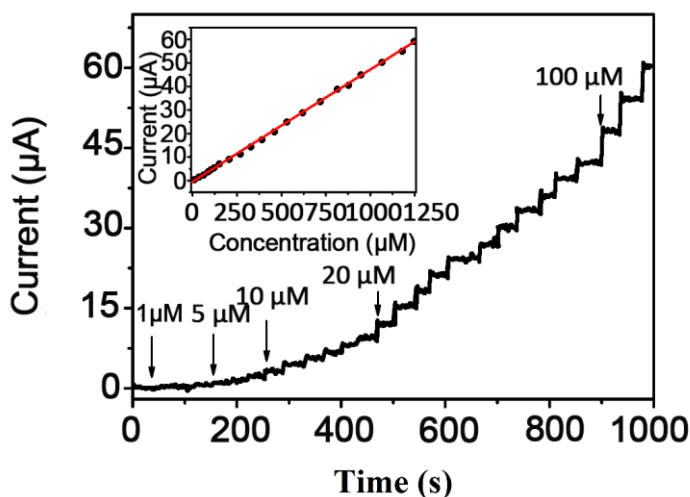

Figure 6. Amperometric response of the CdS NPs/GCE for the successive addition of H_2O_2. Applied potential: 0.62 V. Inset: The calibration curve for H_2O_2 detection using CdS NPs/GCE

The effect of scan rates on the oxidation of 1 mM H_2O_2 in PBS with pH of 7.5 at the CdS NPs/GCE was investigated by CVs. When the scan rate was ranging from 50 to 150 mV/s, the current value of oxidation peak increased gradually with increasing scan rate. The peak currents was related linearly with the scan rates (the regression equation I_{pa} (μA) = 0.5124 v(mV/s) + 28.3669 with R^2 = 0.993). The linear correlation suggested the oxidation of H_2O_2 on CdS NPs/GCE is controlled by adsorption mechanism.

For the H_2O_2 oxidation on CdS NPs/GCE, the response time, linear range and detection limit are of great importance and required to be investigated in detail. Fig. 6 showed the typical amperometric responses of CdS NPs/GCE towards the successive addition of H_2O_2 at potential of 0.62 V. At the moment of adding H_2O_2, the response current increased rapidly and then reached the steady-state within 3 s. Such ultrafast response was resulted from the enhanced electron transfer and electrochemical reaction at the surface of electrode, which could be ascribed to the remarkably conductivity and electrocatalytic property of biosynthesized CdS NPs/GCE. The amperometric responses of H_2O_2 oxidation on CdS NPs/GCE was related linearly with the concentrations of H_2O_2 within the concentration range of 1-1250 μM.

Table 1. Comparison of the present CdS NPs/GCE sensor with other H_2O_2 sensors.

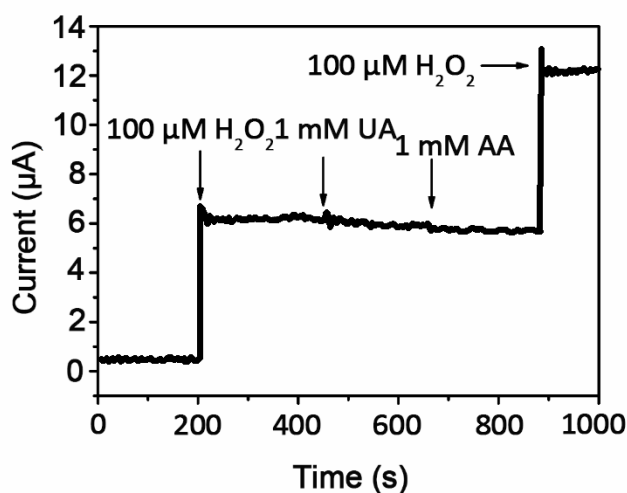| Electrode	Linear detection range	Detection limit	Reference
Ag NPs/ZnO/GCE	0.22 mM to 5.5 mM	0.042 mM	[32]
Cu NPs-CuHCF/ PEDOT/GCE	1 mM to 5.4 mM	0.1 mM	[33]
Hb/C@Au	5 mM to 13.5 mM	0.167 mM	[34]
MnO_2/nafion/GCE	0.01 mM to 0.15 mM	0.002 mM	[35]
Cryptomelane-type manganese oxides/CPE	0.1 mM to 0.69mM	0.002 mM	[36]
CdS NPs/GCE	0.001 mM to 1.25 mM	0.14 μM	This work

Figure 7. Interfering effect of 1.0 mM AA and 1.0 mM UA on the amperometric response of CdS NPs/GCE toward 0.1 mM H_2O_2 in pH 7.5 PBS at 0.62 V.

The regression equation was I_{pa} (μA) = 0.0611 c (μM) − 0.027 with R^2 being 0.995. The calculated detection limit for H_2O_2 was 0.14 μM according to S/N=3. The sensitivity of the CdS NPs/GCE was compared with that of other reported modified electrodes and the results were presented in Table 1. Obviously, the CdS NPs/GCE showed the highest sensitivity owing to the CdS modification, which effectively enhanced electron transferrate.

Chronoamperometry was applied to evaluate anti-interference ability of the CdS NPs/GCE. As to H_2O_2 sensor, the oxidation of other coexist substances including uric acid (UA) and ascorbic acid (AA) was a significant problem. Fig. 7 showed the amperometric response after the consecutive addition of 0.1 mM H_2O_2 and the mixture of interfering species (AA and UA) with the concentration of 1 mM. It can be seen that a well-defined current response of H_2O_2 was still observed despite the addition of AA and UA, suggesting the excellent anti-interference ability of the CdS NPs/GCE.

The reproducibility of the proposed sensor towards 0.1 mM H_2O_2 in PBS was investigated by conducting 10 measurements at exactly same conditions. The RSD values calculated was 4.2%, suggesting the excellent repeatable performance. In addition, the storage stability of the CdS NPs/GCE was also investigated. The current response showed a 2.5% decrease after the CdS NPs/GCE was stored in fridge for 4 weeks, demonstrating the outstanding stability of the proposed CdS NPs/GCE sensor for the determination of H_2O_2.

In an attempt to explore the CdS NPs composite for pritical application, the fabricated sensor was used for determining H_2O_2 in soft drinks. In a typical process, 250 μL soft drink was added into PBS. The current value was then recorded at —0.62 V. Table 2 shows the results of the determinations. The H_2O_2 concentration in two samples is 0.2 mM and 0.5 mM, respectively. The recovery performance of H_2O_2 was deduced using standard addition method. It can be seen that the CdS/GCE shows excellent recovery values. Titanium sulfate colorimetric method was used as a comparison technique for determine the value of H_2O_2 [31], which suggests the CdS/GCE composite is an excellent analytical candidate for H_2O_2 determination.

Table 2. Determination of H_2O_2 in soft drinks using amperometry and control method.

Sample	H_2O_2 value	Added	Found	RSD	Recovery	Titanium sulfate colorimetry
1	0.2 mM	0.1 mM	0.303 mM	3.14%	102.67%	0.301 mM
2	0.5 mM	0.2 mM	0.724 mM	4.24%	102.86%	0.727 mM

4. CONCLUSION

In this report, we proposed a biosynthesis method for CdS NP preparation using yeast, *Saccharomyces cerevisiae*. The synthesized CdS NPs showed an average size of 2.76 nm with high purity. The biosynthesized CdS NPs were then applied as a probe for the detection of DNA using fluorescence measurements. The study showed that CdS NPs performed well in P_{HIV} detection. Based on our study, the biosynthesized CdS NPs can act as an effective sensing platform for fluorescence-

enhanced detection of biomolecules. The GCE modified with biosynthesized CdS NPs demonstrated excellent eletctrocatalytic performance for the determination of hydrogen peroxide. The linear detection range and detection limit of the proposed sensor were found to be 1-1250 μM and 0.14 μM, respectively.

References

1. A. Demming, R. Österbacka and J.-W. Han, *Nanotechnology*, 25 (2014) 090201
2. X. Qu, P.J. Alvarez and Q. Li, *Water. Res.*, 47 (2013) 3931
3. Y. Zheng, L. Fu, F. Han, A. Wang, W. Cai, J. Yu, J. Yang and F. Peng, *Green. Chem. Lett. Rew.*, 8 (2015) 59
4. L. Fu, Y. Zheng, Q. Ren, A. Wang and B. Deng, *Journal of Ovonic Research*, 11 (2015) 21
5. L. Fu and Z. Fu, *Ceram. Int.*, 41 (2015) 2492
6. B.N. Singh, A.K.S. Rawat, W. Khan, A.H. Naqvi and B.R. Singh, *PloS one*, 9 (2014) e106937
7. J. Sarkar, M. Ghosh, A. Mukherjee, D. Chattopadhyay and K. Acharya, *Bioprocess and biosystems engineering*, 37 (2014) 165
8. M. Zheng, Z. Xie, D. Qu, D. Li, P. Du, X. Jing and Z. Sun, *ACS applied materials & interfaces*, 5 (2013) 13242
9. S. Liu, X. Wang, K. Wang, R. Lv and Y. Xu, *Appl. Surf. Sci.*, 283 (2013) 732
10. X. Yang, D. Zhao, K.S. Leck, S.T. Tan, Y.X. Tang, J. Zhao, H.V. Demir and X.W. Sun, *Adv. Mater.*, 24 (2012) 4180
11. Z. Chen, S. Liu, M.-Q. Yang and Y.-J. Xu, *ACS applied materials & interfaces*, 5 (2013) 4309
12. H.N. Abdelhamid and H.-F. Wu, *Journal of Materials Chemistry B*, 1 (2013) 6094
13. Y. Shi, K. Zhou, B. Wang, S. Jiang, X. Qian, Z. Gui, R.K. Yuen and Y. Hu, *Journal of Materials Chemistry A*, 2 (2014) 535
14. J. Jiao, Z.-J. Zhou, W.-H. Zhou and S.-X. Wu, *Mat. Sci. Semicon. Proc.*, 16 (2013) 435
15. J. Barroso, L. Saa, R. Grinyte and V. Pavlov, *Biosensors and Bioelectronics*, 77 (2016) 323
16. J. Frank, A. Pompella and H. Biesalski, *Free Radical Biology and Medicine*, 29 (2000) 1096
17. N.J. Dovichi and J. Zhang, *Angewandte Chemie International Edition*, 39 (2000) 4463
18. F. Liu, J.Y. Choi and T.S. Seo, *Biosensors and Bioelectronics*, 25 (2010) 2361
19. D.P. Negi and T.I. Chanu, *Nanotechnology*, 19 (2008) 465503
20. L. Wang, J. Fu, H. Chen, A. Liang, B. Qian, B. Ling and C. Zhou, *Journal of Luminescence*, 130 (2010) 845
21. W.-W. Zhao, P.-P. Yu, Y. Shan, J. Wang, J.-J. Xu and H.-Y. Chen, *Anal. Chem.*, 84 (2012) 5892
22. C. Yang, M. Li, W.-H. Zhang and C. Li, *Solar Energy Materials and Solar Cells*, 115 (2013) 100
23. E.A. Hunt, A.M. Goulding and S.K. Deo, *Analytical biochemistry*, 387 (2009) 1
24. C.H. Kuo, D.A. Kriz, A. Gudz and S.L. Suib, *Bio-Nanoparticles: Biosynthesis and Sustainable Biotechnological Implications*, (2015) 123
25. D. Singh, V. Rathod, S. Ninganagouda, J. Herimath and P. Kulkarni, *Journal of Pharmacy Research*, 7 (2013) 448
26. A.M. Balu, J.M. Campelo, R. Luque, F. Rajabi and A.A. Romero, *Mater. Chem. Phys.*, 124 (2010) 52
27. G. Wang, W. Chen, C. Liang, Y. Wang, G. Meng and L. Zhang, *Inorganic chemistry communications*, 4 (2001) 208

28. A. Ahmad, S. Senapati, M.I. Khan, R. Kumar and M. Sastry, *Langmuir*, 19 (2003) 3550
29. D.F. Ortiz, T. Ruscitti, K.F. McCue and D.W. Ow, *Journal of Biological Chemistry*, 270 (1995) 4721
30. K. Prasad and A.K. Jha, *Journal of colloid and interface science*, 342 (2010) 68
31. J. Jian, J. Lin, C. Xia, Y. Wen- Sheng and L. Tie- Jin, *Chinese Journal of Chemistry*, 21 (2003) 208
32. Q. Wang and J. Zheng, *Microchim. Acta.*, 169 (2010) 361
33. T.-H. Tsai, T.-W. Chen and S.-M. Chen, *Int J Electrochem Sci*, 6 (2011) 4628
34. W.-L. Zhu, Y. Wang, J. Xuan and J.-R. Zhang, *Journal of nanoscience and nanotechnology*, 11 (2011) 138
35. L. Zhang, Z. Fang, Y. Ni and G. Zhao, *Int. J. Electrochem. Soc*, 4 (2009) 407
36. Y. Lin, X. Cui and L. Li, *Electrochemistry Communications*, 7 (2005) 166